RSC Advances

ROYAL SOCIETY OF CHEMISTRY

www.rsc.org/advances

RSC Advances

RSCPublishing

ARTICLE

A generic microfluidic biosensor of G protein-coupled receptor activation – impedance measurements of reversible morphological changes of reverse transfected HEK293 cells on microelectrodes

Cite this: DOI: 10.1039/xoxxoooooox

Received ooth July 2014,
Accepted ooth July 2014

DOI: 10.1039/xoxxoooooox

www.rsc.org/

Saurabh K. Srivastava,[a,b] Rajesh Ramaneti,[c] Margriet Roelse,[a] Hien Duy Tong,[c] Elwin X. Vrouwe,[d] Aldo G.M. Brinkman,[e,f] Louis C.P.M. de Smet,[e,f] Cees J. M. van Rijn,[b,c] Maarten A. Jongsma,[a,f]

Impedance spectroscopy of cell lines on interdigitated electrodes (IDEs) is an established method of monitoring receptor-specific cell shape changes in response to certain analytes. Normally, assays are done in multiwells making it a bulky, static and single use procedure. Here, we present a biosensor allowing sequential application of biological test samples with an automated microfluidic system. It is capable of monitoring relative changes in impedance using castellated IDEs of 250–500 µm diameter, covered with stable or reverse transfected HEK293 cells. Reversible activation of the Neurokinin 1 (NK1) receptor in stable cell lines was observed in response to a series of 5 minute exposures from 1 pM – 10 nM of the specific ligand Substance P (SP) using impedance measurements at 10 mV and 15 kHz. An optimal flow speed of 10 µl/min was chosen for the 10 µl flow cell. The EC_{50} of ~10 pM was about 10 times lower than the EC_{50} based on measuring changes in the calcium ion concentration. The method was also shown to work with reverse transfected cells. Plasmid DNA encoding the NK1 gene was spotted onto the electrodes and pre-incubated with a transfection agent. The overlaid HEK293 cells were subsequently transfected by the underlying DNA. After challenge with SP, the cells induced an activation response similar to the stable cell line. The microfluidic micro-electrode reverse transfection system opens up possibilities to perform parallel measurements on IDE arrays with distinct receptors per IDE in a single flow channel.

Keywords: G protein-coupled receptor, HEK293 cells, Impedance spectroscopy, Cell based biosensor, Microfluidic flowcell, Interdigitated castellated electrodes.

Introduction

The use of label-free sensing in cell-based screening is gaining increasing interest as a tool to enable the discovery of analytes specific for G Protein-coupled receptors (GPCRs) in applications involving pharmaceutical drug screening.[1,2] A strong potential exists to use these receptors as well for monitoring of food quality and safety, and disease diagnosis. However, the microtiter plate-based platforms tend to be too costly for these tasks.[3,4] Responses of live cells expressing GPCRs to specific analytes are usually immediate, transient (1-5 mins) and can be highly sensitive (nM–pM range). In comparison to conventional diagnostic methods for example PCR for DNA/RNA detection and ELISA for immunodetection, the activation of GPCRs identify a sample's bioactivity, but not its identity. This can be an advantage when the potential ligand is unknown or diverse.[5] Broader application of GPCR-based assays for diagnostics will hinge on our ability to scale down the assays to save on handling and material costs and to integrate them with automated microfluidic formats allowing multiple sequential use and internal calibration.[6]

GPCRs play important roles in sensory, physiological and disease-related signalling processes. As such they can be utilized for screening assays in both medical and food related industries. Collectively the ~800 receptors known in humans specifically recognize extracellular stimulants ranging from glycoproteins, cytokines, hormones, neurotransmitters, growth factors, to tasting and odorant molecules.[7] Once activated, the

dissociating G proteins trigger one or more pathways that finally generate an intracellular response.[8] Generally, for measurement of GPCR activation assays, concentration dynamics of secondary messengers like Ca^{2+} and cAMP are studied in real time utilizing various fluorescent indicator dyes.[9,10] Alternatively, field-effect transistors, impedance spectroscopy, light-addressable potentiometry, patch clamp and piezoelectric methods have been used.[11] Impedance spectroscopy is a well-established technique for studying effects of biomolecules on a wide range of prokaryotic and eukaryotic cells.[12] The technique measures the combined resistive and capacitive changes due to morphological or mass redistribution changes of cells on electrodes.[13, 46]

Yu et al. (2006) showed for the first time that impedance measurements of cells transfected with different GPCRs allowed measurements of morphological changes; however, those were measured in terms of hours rather than minutes.[14] Since then, the advent of dedicated instruments has opened a large research field, and dedicated assays were demonstrated to be similarly sensitive as label-based methods, but operate on a scale of minutes rather than seconds.[1,2] In 2009 Meshki et al. demonstrated substance P (SP)-dependent activation of the $G_{\alpha 12/13}$ pathway using HEK293 cells expressing the NK1 receptor.[15] The pathway causes apoptosis-independent cellular blebbing, and is mediated by the *Rho/Rho*-associated coiled-coil kinase pathway.[15] The activation of this receptor has been associated with the transmission of stress signals and pain, the contraction of smooth muscles and inflammation.[16] The morphological changes of the cells after the activation of the $G_{\alpha 12/13}$ pathway could be monitored using impedance spectroscopy, and there have been similar demonstrations for other receptors and activation pathways.[14,17-19, 47] In general, it is thought that also activation of $G_{\alpha s}$, $G_{\alpha i/o}$ and $G_{\alpha q/11}$ pathways can lead to changes in actin and myosin complexes of the membrane cortex that are essential for cell shape and locomotion.[20]

At present there are four commercial electric cell-substrate impedance-sensing (ECIS) platforms available in the market (ECIS, xCELLigence (RT-CES), Bionas Discovery 2500, Cellkey). These systems have been utilized for a large variety of studies, including cell adhesion, proliferation, cytotoxicity, receptor-mediated signalling, barrier function and immune cell signalling.[21,22] These systems utilize interdigitated electrodes (IDEs) of similar dimensions (i.e. electrode features of 30 microns and line gap of 50 μm)[23] in 8, 16, 96 or 384 (RT-CES and Cellkey) well microplate formats. However, other IDE dimensions are needed to expose cells transiently and/or repeatedly to a ligand, including integration with microfluidic auto-samplers. These changes would make them amenable to automated internal calibration and create possibilities of screening or monitoring of biological targets with lower material and labor costs.[6,24,25] To also match the power for parallel measurements solutions are needed to generate and read cell arrays in flow cells. Some approaches have focused on top down dispensing methods of transfected cells into semi-open array structures.[26] A potentially more elegant and low cost solution can be found in reverse transfection of spotted plasmid DNA.[27] This method allows the formation of cell arrays by overlaying the DNA arrays with a single cell type. However, until now, the method has not been applied to IDE based methods or flowcells.[27]

In this study, we aimed to demonstrate for GPCRs the possibility of doing sequential impedance measurements on stable cell lines and reverse transfected cells by monitoring impedance changes during serial injections of analyte in a microfluidic flow configuration.

Materials and Methods

Materials

All chemicals were analytical grade and supplied by Sigma Aldrich, unless specified otherwise. The NK1 receptor gene construct NK1-T2ANC YC3.6 for stable and reverse transfection cell lines as well as the cell culture conditions were as described by Roelse et al.[28] All solutions were prepared in demineralized water (conductivity 18.2 MΩ·cm) obtained using Pure lab Ultra from Elga Lab solutions.

IDE preparation

The gold IDEs were fabricated (Nanosens BV, Zutphen NL) using a standard micro-photolithography process on thermally oxidized silicon oxide/silicon substrates of 10 × 15 mm dimensions. Interdigitated chromium-gold patterns of 20 μm line width with castellated features of 40 μm length and a line spacing of 12 μm were printed on the silicon substrates as a series of 5 sensing electrodes with a unit-to-unit distance of 500 μm, and electrode dimensions of 500 × 500 (central three) or 250 × 250 μm (terminal two) (Figure 1A). Prior to use, the sensing chips were subjected to cleaning, surface activation and modification procedures. New and used IDE sensor chips were cleaned with 2% Hellmanex II in MilliQ water followed by exposing the chips to a 2% HF solution for 10 sec and rinsing with demineralized water. For adherence of cells, surface functionalization of both gold and silicon oxide (SiO_2) was required. First, the gold electrodes were surface functionalized via drop casting with 25 mM of cysteamine in ethanol for 30 min[29] followed by a modification of the SiO_2 surface with APTES through chemical vapor deposition on the chip.[30] Subsequently, the gold arms connecting the sensing area with the contact pads were covered with a negative photoresist SR3170 PR. Finally, bovine fibronectin (100 μg/ml, Mw ~220 kDa) was drop-casted, incubated for 30 min at 37 ºC, and unbound fibronectin was rinsed off the chips with MilliQ water.[29,31]

Flowcell set up

A re-sealable and re-usable flow cell was designed to allow connection to a microfluidics system. The flow cell had dimensions of 4.5 cm × 1.5 cm × 0.15 cm. On the top of the borosilicate glass flowcell the in- and outlets were spaced 3.5 cm apart and on the downside 4 mm apart, connected by an

internal microfluidic channel. A poly-silicone gasket of 5 mm in diameter and 1 mm in height yielded a compact encasing around the 5 IDEs and resulted in a flow cell volume of 10 µl. The fluids were supplied to the inlets through a Teflon connection tubing of inner diameter 250 µm while the outlet tubing had an internal diameter of 750 µm to prevent any pressure build-up and leakage from the flow cell. The design is available in the online version of the PhD thesis http://edepot.wur.nl/324299 Chapter 6.

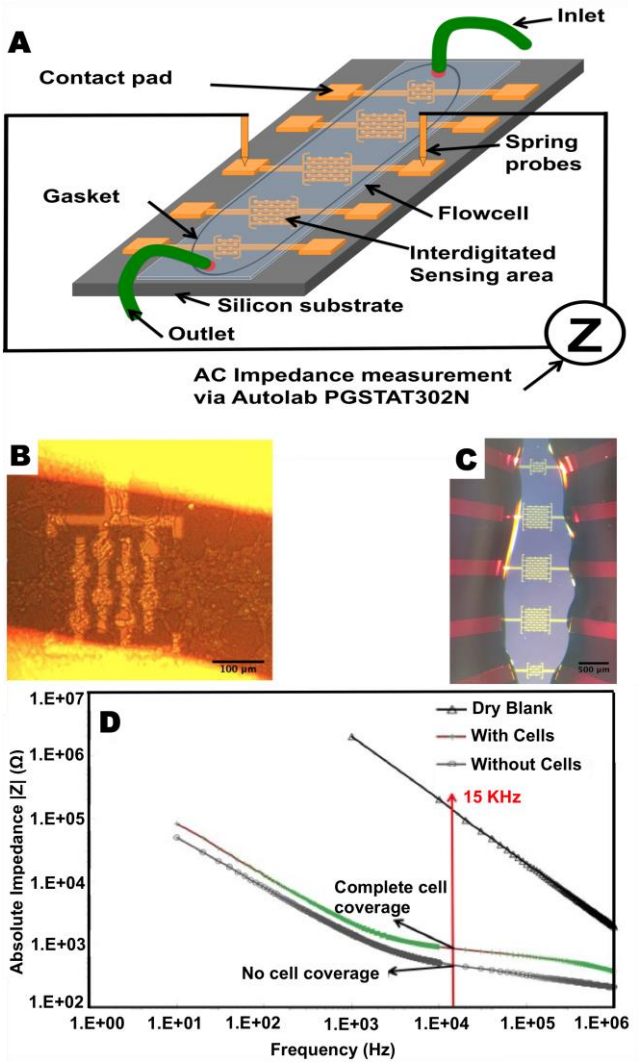

***Fig 1**: Optical and electrical characterization of IDE electrode chips. A: Schematic representation of the sensing device. B: Microscopic image of a 250 µm IDE coated with NK1-HEK293 cells[28] showing a ~80% coverage on the electrode between the yellow layers of photoresist after the measurement. C: Microscopic image of an IDE chip between the yellow layers of photoresist before cell coating. D: A Bode impedance spectrum of an IDE of 500 µm with and without cell coverage in HEPES buffer or without liquid medium exposed to ambient air (dry blank). The indicated 15 kHz was chosen as test frequency in later experiments.*

Cultured chips were placed in a tailor made stainless steel chip holder of dimensions of l × b × h: 8 cm × 5.5 cm × 0.56 cm with slot dimensions for placing the flow cell of 4.5 ± 0.03 cm × 1.5 ± 0.03 cm × 0.39 cm, and with slot dimensions for placing the sensing device of 1.5 ± 0.03 cm × 1 cm × 0.17 cm (Micronit Microfluidics BV, Enschede, NL). A printed circuit board (PCB) with solder-mounted spring probes for connection to the sensing device was assembled over the chip holder. This flow cell device was mounted inside a die-cast aluminum metal alloy LM24 Faraday cage to exclude environmental noise from light and external electromagnetic interference and enable easily accessible connections to the signal readout systems.

IDE preparation with stable cell lines and reverse transfected cells

The fibronectin coated IDE chips were seeded and incubated for 15 min with 0.5 ml of freshly harvested NK1 expressing stable HEK293 cell lines[28] by drop casting at either a density of 1×10^4 or 1×10^6 cells/ml, followed by the addition of 9.5 ml of freshly prepared DMEM medium in a dish of 5.5 cm in diameter. A uniform monolayer of cells with ~50% coverage for lower and ~80-100% for higher seeding density had formed after 48 h of incubation at 37ºC in a 5% CO_2 environment. All subsequent experiments were performed at room temperature in HEPES assay buffer composed of 20 mM HEPES pH 7.4, 137 mM NaCl, 5.4 mM KCl, 1.8 mM $CaCl_2$, 0.8 mM $MgSO_4$ and 20 mM glucose. Serial injections of various freshly prepared dilutions of NK1 ligand Substance P (Bachem AG, Switzerland, product nr. H-1890, stock solution of 0.5 mM (0.67 mg/ml in 50% acetic acid) in HEPES assay buffer were carried out at a constant flow rate of 10 µl/min.

For reverse transfection experiments fibronectin-modified chips were used as described above. The 0.5 mm diameter sensing area of the IDE was spotted with 1 µl of DNA-gelatin mixture (1 µg of transfection grade NK1-T2ANC YC3.6 as described by Roelse *et al.*[28] with 1 µl of 1.5 M sucrose and 12 µl 1% gelatin in total of 30 µl MilliQ) using a micropipette, followed by drying for 1 h in a 50–60% humidity chamber. Spotted chips were stored in a dry box. For experiments, the chips were drop casted with 30 µl of effectene mixture (30 µl of buffer EC, 3.2 µl of enhancer and 5µl of effectene reagent, all taken from the Qiagen effectene transfection kit) on top of the DNA spotted area and incubated for 10¬20 min at room temperature. The chips were then rinsed with DMEM medium and seeded with freshly harvested wild type HEK293 cells at a density of either 1×10^4 cells/ml (the multiple loop injections of 1 nM SP experiment) or 1×10^6 cells/ml (the multiple-loop injections of 1 pM to 100 pM SP experiment) and cultured in DMEM medium for 48 h in an incubator with 5% CO_2 at 37ºC.

Impedance measurements

Impedance measurements were performed at a fixed voltage of 10 mV and a fixed frequency of 15 kHz as described previously 32 and cell responses were measured as a function of time using an Auto Lab PGSTAT302N with FRA2 module (Metrohm Autolab B.V., The Netherlands) at a frequency

interval of 3 s. The sensitivity of the instrument was in the range of ~0.1 Ω±2% – 1 Ω±0.3%. Before and after each series of measurements a frequency-impedance sweep of the cell covered electrode and the bare electrode was carried out in the range of 1 Hz to 1 MHz in order to quantify the impedance contributed by the cells covering the IDEs.

Results

Impedance characterization of cell covered IDEs

To allow experiments in the flow cell the first requisite was proper adhesion of the cells to the gold electrodes under the shear of the applied flow rate. For this, IDE chips were given a surface modification using cysteamine, APTES and fibronectin to enhance cell adhesion under flow as described in Materials and Methods. Stable NK1 receptor expressing HEK 293 cells (1×10^6 cells/ml) were applied on the IDEs and after 2 days of culturing a nearly complete monolayer of cells was formed (Figure 1B). After the flow cell was integrated into the stainless steel chip holder, a flow of 10 µl/min was applied. The absolute impedance response as a function of frequency sweep (Bode plot) was recorded for both cell-covered (Figure 1B) and cell-free IDEs (Figure 1C) in a set up as shown in Figure 1A. Absolute impedance was found to in-crease in the range of 100Hz to 1MHz due to the coverage of cells on the electrodes. For time-dependent measurements we chose to work at a frequency of 15 kHz where electrode surface-related effects are dominant and the cells induced an additional impedance of around 2 kΩ for 500 µm IDEs (Figure 1D), and 2.5 kΩ for 250 µm IDEs.

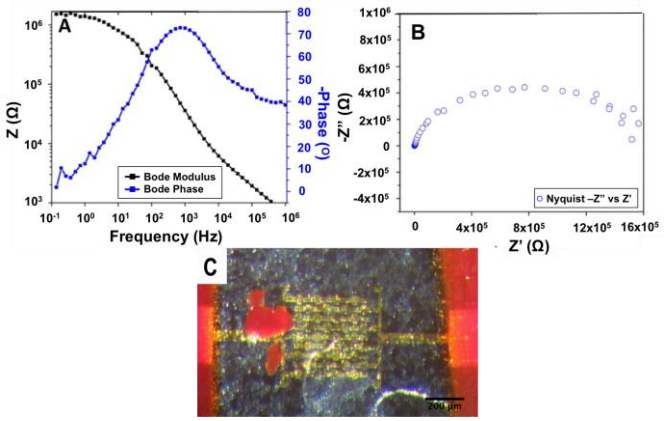

***Fig 2**: Optical and electrical characterization of a 500 µm IDE with stableNK1 HEK293 cells. A: Bode plot of an IDE covered with NK1-HEK293 cells. The black line indicates the impedance, and the blue line shows the phase. B: Nyquist plot of the same IDE. C: optical microscope image with normal light of a cell covered microelectrode of 500 µm after the experiment. In red is the photoresist (SR3170 PR) shielding the connecting electrodes from the assay solution. The plots were obtained from the central 500 µm electrode.*

Prior to further analysis each electrode, covered with stable NK1 receptor expressing HEK293 cells, was first characterized with a Bode plot (Figure 2A) and a Nyquist plot (Figure 2B). The Bode plot was generated under a 10 µl/min flow of HEPES medium. At around 1 kHz, the phase shift of the Bode plot reached a maximum of around 70°, which was indicative of a quasi-capacitive behaviour originating from the nearly confluent cell layer on the electrode, which slowly decreased upon increasing frequency.[33,34] In the sample analysed in Figure 2B, the Nyquist plot shows a quasi-parallel resistive-capacitive RC component behaviour for the central cell-covered electrodes (500 µm) (Figure 2B and 2C).[34]

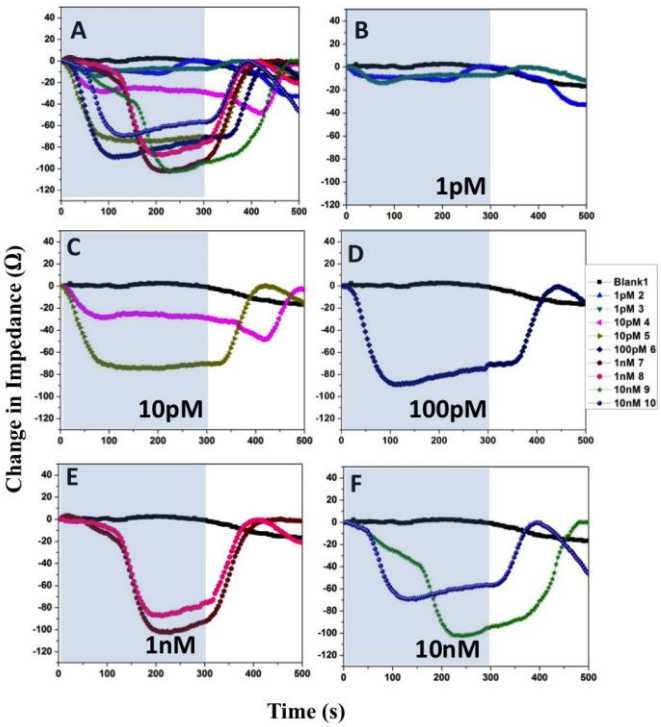

***Fig 3**: Impedance change of a 500 µm IDE covered with an stable NK1 receptor expressing cell line in response to 300 s injections of different concentrations of ligand SP. Panel A: the combined data of impedance response to different concentrations of ligand doses ranging from 1 pM to 10 nM on interdigitated electrodes covered with stable NK1 receptor expressing cells. Panels 3B-3F: the changes in impedance for individual ligand dose concentrations. The intervals in light blue background colour represent the period that SP was contacting the cells, while areas in white represent recovery periods with buffer flow without ligand. The notation 1–10 in the ligand of the plot represents the sequence of injection. Assay-independent drift was corrected in all cases by subtracting a linear slope coefficient of a line drawn between t = 0 and the highest recovery point between t = 400–500 s post injection (t = 300 s for the blank).*

Impedance responses of stable NK1 receptor-expressing HEK293 cells to SP

Based on the response obtained from impedance spectra of the Bode and Nyquist plots (Figure 2), a single pair of 500 µm IDEs covered with stable NK1 receptor expressing cells was chosen to measure the specific cell response to activation by a series of injections of SP. Following literature and from Figure 1, a frequency of 15 kHz and amplitude of 10 mV was chosen to record the induced changes in cell-electrode coverage.[32,35] A 50 µl sample of SP was loop-injected at concentrations ranging

from 1 pM to 10 nM. Samples were diluted in the same HEPES buffer also used for continuous flow. Due to the constant flow rate of 10 µl/min each 50µl injection lasted 5 minutes and was always followed by a recovery period of at least 2–3 minutes. As a control for non-specific buffer effects or drifts from switching the valve, blank injections were done by injecting only buffer on stable NK1 receptor expressing cells (Figure 3).

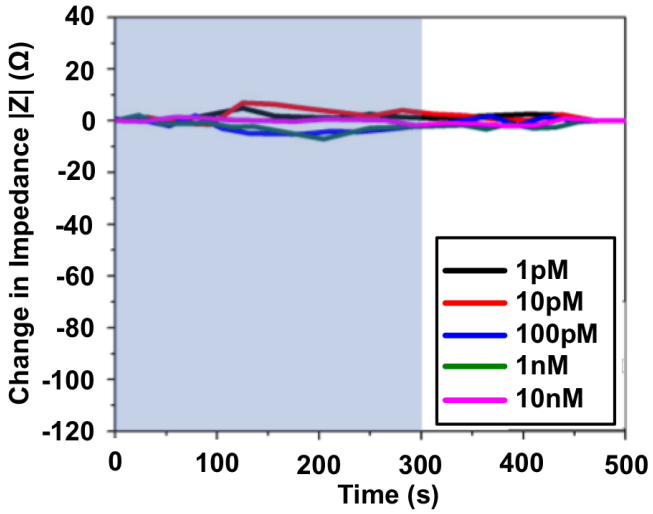

***Fig 4**: Transient response of wild type HEK293 cell lines coated IDEs (500 µm) to the SP ligand (1 pM-10 nM). Assay-independent drift was corrected as in Fig 3.*

As a negative control to verify that the signals obtained were due to GPCR activation only and not due to changing concentrations of SP, different concentrations of SP were tested on wild type HEK293 cells (Figure 4). In detail, Figure 3A shows the combined signals obtained from stable NK1 receptor expressing covered electrodes during and after exposure to 1 pM to 10 nM SP as a function of time. Subplots of Figure 3B-3F show the same for individual SP concentrations compared to the blank measurement. The overall sample resistance of the sensing area coated with cells was around ~5 kΩ with a contribution from cells of ~2 kΩ. The baseline noise level was below ~2 Ω for this sample. The system could detect cell morphological changes after challenges with concentrations of SP down to 1 pM even when the electrodes were fully covered with cells. An average impedance change of around 14 Ω was observed for 1 pM concentrations, whereas the higher concentrations (10 pM, 100 pM, 1 nM and 10 nM) showed average changes of 60, 89, 94 and 87 Ω, respectively. Impedance changes associated with the mechanical injection process were found to be negligible. Every injection of SP followed a typical response pattern, with a maximum response being reached typically 100–200 sec after injection, followed by decreasing impedance and a recovery period after removal of SP of again 100–200 sec. The activation and recovery slopes of the curves were very similar, independent of the ligand concentration, but the response valleys were deeper at higher ligand concentrations. There was some uncontrolled variation in both the onset (e.g. Figure 3E and F) of the strong response and also in the response duration (e.g. Figure 3E vs. the rest). These irregularities might be explained by fluctuations in the flow due to the very small displaced volumes. As a result samples appear to be delivered later (3EF) and/or faster (3E) than calculated. Also the tenth injection of 10 nM SP, showed a lower response compared to the ninth injection of the same concentration of SP. This is very likely be due to saturation of the receptor as described by Roelse et al. 2013.[28]

Impedance responses to SP on NK1-expressing reverse transfected wild type HEK293 cells

Arrays of electrodes in a single flow cell can be individually transfected with different receptors by means of reverse transfection. HEK293 cells, reverse transfected with NK1 plasmid DNA on 500 µm electrodes, were first characterized with Bode (Figure 5A) and Nyquist (Figure 5B) plots when full cell coverage was reached after 48 h. These plots were generated under a 10 µl/min flow of HEPES medium and the phase response was plotted for reference purposes. Two-phase shifts at 1–15 kHz, and 0.1–1 Hz were evident in the Bode plot (Figure 5A) suggesting two independent electrical Resistance-Capacitance circuits (RC circuit). This is also evident in the Nyquist plot (Figure 5B) where two corresponding semicircular regions are observed. The large semicircle corresponds to a low frequency RC-circuit formed by the internal IDE electrical capacity and an electrical resistance, originating from the transport/diffusion of ions via the bulk liquid towards the electrodes. The small semicircle corresponds to a second RC-circuit formed by the electrical capacity of the cell-envelopes and the electrical conductance within the cells and of the exo-ions towards the electrodes. Both RC circuits are present in parallel (cf. extended Randle equivalent circuit) and at 15 kHz mainly the presence of the second RC-circuit is probed, herewith recording sensitive changes in the electrical capacity of the cell-envelopes.

To test the compatibility of the process of reverse transfection with impedance measurements, two distinct experiments were performed. First, doses of 1 nM SP were repeatedly passed over reverse transfected cells with chips seeded at a lower cell density (1×10^4 cells/ml), and after that, doses ranging from 1–100 pM SP were tested on a different chip seeded at high cell density (1×10^6 cells/ml). Figure 6A shows the combined signal obtained from reverse transfected cell-covered electrodes exposed to repeated 1 nM SP injections. An average maximum response amplitude of ~18 Ω was obtained which was 2–3 Ω less than the signal obtained for 1 nM with stable transfected NK1 cell lines seeded at the same cell density of 1×10^4 cells/ml (data not shown), but ~76 Ω less compared to electrodes seeded with 100 times more cells. Transient response curves were different from the shapes obtained with stable cell lines as the deepest point of the curve was usually reached after removal of SP. The apparent decrease in the signal response (slope and depth) in the later two injections (-5 and -6) may be attributed

to temporary desensitization of the NK1 receptor cells due to receptor recycling of SP-activated receptors.[28]

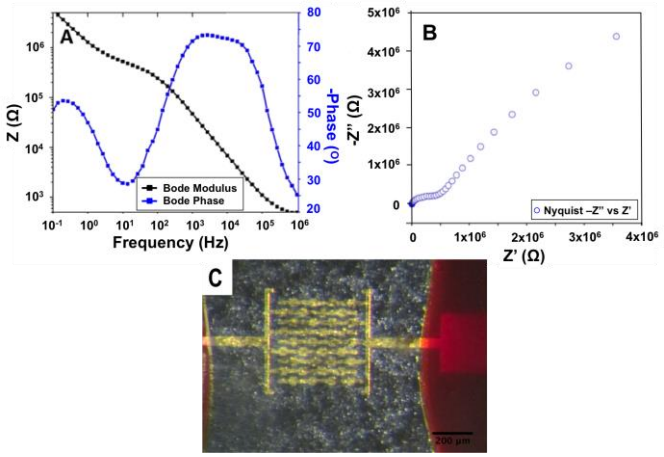

***Fig 5**: Optical and electrical characterization of IDE (500 µm) electrode chip used for the experiments with reverse transfected HEK293 cells expressing NK1 receptor. A: Bode plot from an electrode covered with reverse transfected HEK293 cells expressing NK1 receptors. B: Nyquist plot from a cell-covered electrode and C: optical image of cell-covered electrodes of 500 µm. In red is the photoresist (SR3170 PR) covering the thick connecting electrodes.*

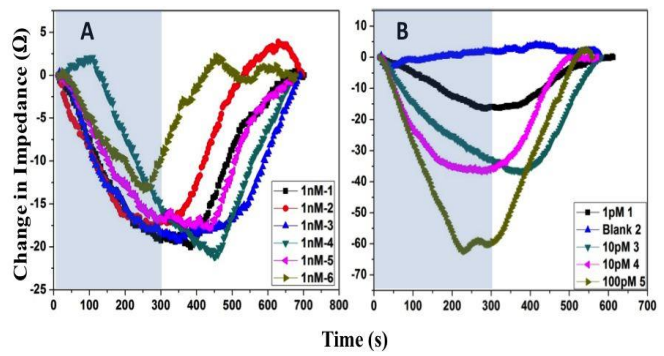

***Fig 6**: Transient response of NK1 reverse transfected HEK293 cell lines on 500µm IDE's to the SP ligand. A: shows the combined data of the impedance response as a result of a series of injections of 1nM SP on reverse transfected HEK293 cells with NK1 plasmid DNA at cell seeding density of 1×10^4 cells/ml, the sequence of injection is represented by the notation 1–6 in the legend of the plot, where 1 represents the first injection while 6 represents the last injection. B: shows the combined data for impedance response with different concentrations of ligand doses ranging from 1 pM to 100 pM on interdigitated electrodes covered with reverse transfected NK1 HEK293 cells at cell seeding density of 1×10^6 cells/ml. The notation 1–5 in the legend of the plot represents the sequence of injection. Assay-independent drift was corrected as in Fig. 3.*

In the second experiment a different single pair of IDE electrodes covered with NK1 reverse transfected HEK293 was selected to measure the signal responses to doses ranging from 1 to 100 pM SP. The overall sample resistance for all the cell covered electrodes on different chips were in the range of 4–4.5 kΩ with baseline noise level of 2 Ω. The change in absolute impedance for 1 pM SP was similar to the stable NK1 expressing HEK293 cells (~16 Ω). For higher concentrations of 10 and 100 pM, the average impedance changes were 37 and 62 Ω, respectively (Figure 6B). No significant impedance changes were observed in the blank experiment with no SP in HEPES media.

Discussion

Multiwell assays are the basis of the current impedance- and molecular probe-based analytical platforms of measuring specific cell or receptor responses.[15,36,37] These static assays are relatively costly, (labor and reagent intensive), wasteful (single use only), and with a relatively low information content (only on-rates of compound addition, no off rates of compound removal, no internal calibration with injection of a standard).[38,39] In view of the demand for smaller, parallel, multiple use, dynamic fluidic assays, we therefore developed a prototype system potentially combining all these desirable traits. The system consists of a flowcell enclosing multiple interdigitated micro-electrodes that can be specifically reverse transfected with DNA plasmids encoding different cell membrane receptors to create receptor cell arrays. DNA-printed electrodes can be stored for months until use and the cell arrays can be addressed repeatedly due to the reversible nature of the morphological changes. In addition, the transient activation provides the kinetic profile of both activation and de-activation at the level of changes in cell morphology.

Current limitations of the system prototype are: (i) Due to electrode interference during simultaneous measurements the technical set up did not allow reading more than one sensing electrode. Systems sequentially addressing electrodes at intervals have been developed for the existing microtiter plate formats, however, so that we do not foresee a technical hurdle for flow cell arrays; (ii) the design of the flow cell did not allow higher flows than one flowcell volume per minute. Future designs with wider and/or higher flow cells will allow larger flow volumes as described by Roelse et al. with greater convenience in terms of the speed of delivery of series of samples;[28] (iii) The non-monotonous drift could not be addressed in the present system with a read out of only a single receptor. Drift compensation methods need to be realised by adapting the design of the chip layout for example by arranging a rows-column format with electrical connections lying plane perpendicular and at the underside of the sensing area thereby minimizing the chances of drift due to thermal and electrical interferences from neighbouring electrodes.[40] If drift is IDE independent compensation may also be achieved by subtracting the signals of control electrodes. If drift is IDE dependent the process of cell division may be responsible. The mitotic cycle induces strong morphological changes that likely disturb signal stability on small electrodes with only few cells contributing to

the total signal. Arresting the cell cycle with chemicals may therefore be another effective way of suppressing drift.

HEK293 cells were seeded on the chip typically 48 h prior to use. Depending the chosen cell densities, this yielded well-attached, uniform, 50-100% confluent cell layers. Loading higher densities and spinning cells down to reduce the adhesion time from 48 h to < 2 h was not effective, as cells could not withstand medium flow speeds higher than 2 µl/min, due to poor adherence (data not shown). It is noted that the morphological changes of cells can involve both shrinking and stretching, depending on the nature of the activated receptor.[41,42] This probably has some implications for the most adequate cell coverage in case of mixed cell responses. In the present study the NK1 receptor activation with SP resulted in shrinkage of cells (blebbing), and therefore, near confluent cell coverage yielded the best differential signal. In a mixed situation it may be better to aim for 70–80% cell coverage, in order to allow for efficient measurements of cell stretching.

The signal responses obtained with various ligand doses were generally reproducible for both stable as well as reverse transfected cell lines. Noise levels were typically 2~5 % relative to response signals of ~20 Ω and higher. The response profiles of stable and reverse transfected cell lines were, however, a little different. Stable cell lines displayed an initial 1–2 minute steep decrease followed by a 3–4 minute slightly rising saturation plateau, succeeded by a 1–2 minute steep rise when the ligand was removed. Both the fall and rise of the signals could be delayed up to 100 s. We suspect that this might be due to failure of the pump to deliver a constant low flow in our system. By comparison for reverse transfected cell lines the decrease was less steep, taking 4–5 minutes to reach a shorter, yet still decreasing, saturation plateau, which would extend 1–2 minutes beyond the point that the ligand was removed. Recovery was also slower taking up to 4–5 min. A possible explanation might be that HEK293 cells were present in a multilayer, with only the lower layer being transfected and responding. In comparison to uniform stable transfected cell lines, the ligand may reach the bottom reverse transfected cells less efficiently.

From our results we estimate an EC_{50} value of ~10 pM, which is 140 times lower compared to the EC_{50} reported by Meshki *et al.*[15]. Experiments in a microtiter plate on large electrodes[15] and about 10 times lower than a complementary microfluidic system where cyto-plasmic [Ca^{2+}] changes were measured.[28] One reason for this higher sensitivity could be the very low cell density used by Meshki et al. in the wells, i.e. 4000 cells/6.4 mm well diameter.

Based on a cell size of 100 µm^2 these results in coverage of only 1.25% compared to 80-100% coverage in our sample preparations. This was also evident with the experiment involving repeated injections of 1 nM, where the signal obtained was diminished for lower cell inoculation of 10^4 cell/ml compared to higher cell inoculation 10^6 cells/ml. In addition, we incubated cells 3 times longer (48 h) allowing stronger electrode adhesion of cells. Secondly, the reported lower sensitivity values from Meskhi et al. could be due to SP not being fully active as it quickly inactivates after dilution in buffer according to our experience. Thirdly, considering the mean cell size (10 µm), the line spacing used in our case was very narrow (12 µm) com-pared to commercial devices (50 µm) used by Meshki et al.[15] As described by Radke and Alocilja, for sensitive impedance measurement of cellular organisms, an electrode spacing should be proportional to the dimensions of cells,[43] so as to minimize the influence of events occurring due to some random particle floating over the sensor electrode. In their study where they utilized *E. coli* bacteria with average length of 2.5 µm, the optimum spacing between the electrodes was 4 µm which minimized up to 98% of external interference caused by random particles floating at a distance of 10 µm over the sensing area.[43]

For proof of concept, the NK1 receptor was utilized as a model GPCR. Upon activation by SP, the NK1 receptor triggers both the $G_{\alpha q}$ and the $G_{\alpha 12/13}$ pathways. $G_{\alpha 12/13}$ mediates a shrinking cell shape due to the contraction of the cell cortex.[15] There have been similar demonstrations, however, for the histamine (H1), serotonin (5-HT1A) 14, dopamine (D2, D5), cannabinoid 1 (CB1), melanocortin-4 (MC4R),[17] cannabinoid 2 (CB2), metabotropic glutamate 1 (mGluR1)[18] and chemokine CXCR3[19] receptors with activation pathways mainly involving $G_{\alpha s}$, $G_{\alpha i/o}$ and $G_{\alpha q/11}$. Furthermore, also the ligands of nuclear receptors such as glucocorticoid, mineral corticoid, progesterone, androgen receptor induce morphological changes in cells.[44] The presented novel microfluidic system of impedance measurements on microelectrodes in a flow cell is therefore potentially useful for a much wider array of receptors. In fact, if they do not naturally change shape, their signalling pathway can be altered in order to do so. Recently, $G_{\alpha q}$ proteins could be engineered into chimeric versions with $G_{\alpha 12/13}$, which would bind $G_{\alpha q}$ GPCRs, but trigger the $G_{\alpha 12/13}$ pathway,[45] thus opening up further possibilities to use impedance measurements as a truly generic platform for G-protein-coupled receptor research.

Acknowledgements

The authors acknowledge Hans Meijer and Harrie Verhoeven for fabrication of the module, and Metrohm Autolab B.V., The Netherlands for providing the Autolab Instrument for the experiments. Financial support for SKS was obtained from the Dutch Technology Foundation STW (Project 10058) (SV). MJ was supported by the Nano4Vitality program 2008-I and, just like AGMB and LCPMdS by NanoNextNL, a micro- and nanotechnology consortium of the Government of the Netherlands and 130 partners.

[a]Plant Research International, Wageningen UR, Droevendaalsesteeg 1, 6708 PB Wageningen, The Netherlands
[b]Laboratory of Organic Chemistry, WageningenUR, Dreijenplein 8, 6703 HB Wageningen, The Netherlands
[c]Nanosens B.V., Berkelkade 11, 7201 JE Zutphen, The Netherlands
[d]Micronit Microfluidics B.V., Colosseum 15, 7521 PV Enschede, The Netherlands

[e]Department of Chemical Engineering, Delft University of Technology, Julianalaan 136, 2628 BL Delft, The Netherlands
[f]NanoNextNL, P. O. Box 3021, 3502 GA Utrecht, The Netherlands

Dr. Maarten A. Jongsma; Plant Research International, Droevendaalsesteeg 1, Wageningen University, 6708 PB Wageningen, The Netherlands. Email: maarten.jongsma@wur.nl; Tel: +31-317-480932; Fax: +31-317-418094.

References

1. C. W. Scott and M. F. Peters, *Drug Discov Today*, 2010, **15**, 704-716.
2. Y. Fang, A. G. Frutos and R. Verklereen, *Comb Chem High Throughput Screen*, 2008, **11**, 357-369.
3. I. Beets, M. Lindemans, T. Janssen and P. Verleyen, *Methods Mol Biol*, 2011, **789**, 377-391.
4. R. Lappano and M. Maggiolini, *Nat Rev Drug Discov*, 2011, **10**, 47-60.
5. X. Cheng, G. Chen and W. R. Rodriguez, *Anal Bioanal Chem*, 2009, **393**, 487-501.
6. S. A. Martins, J. R. Trabuco, G. A. Monteiro, V. Chu, J. P. Conde and D. M. Prazeres, *Trends Biotechnol*, 2012, **30**, 566-574.
7. R. Zhang and X. Xie, *Acta Pharmacol Sin*, 2012, **33**, 372-384.
8. E. Hermans, *Pharmacol Therapeut*, 2003, **99**, 25-44.
9. M. J. Berridge, M. D. Bootman and H. L. Roderick, *Nat Rev Mol Cell Bio*, 2003, **4**, 517-529.
10. R. M. Paredes, J. C. Etzler, L. T. Watts, W. Zheng and J. D. Lechleiter, *Methods*, 2008, **46**, 143-151.
11. P. L. Wang, Q., *Cell-Based Biosensors: Principles and Applications*, Artech House Series, Norwood, MA 2010.
12. E. P. Randviir and C. E. Banks, *Anal Met*, 2013, **5**, 1098-1115.
13. L. Ding, D. Du, X. J. Zhang and H. X. Ju, *Curr Med Chem*, 2008, **15**, 3160-3170.
14. N. Yu, J. M. Atienza, J. Bernard, S. Blanc, J. Zhu, X. Wang, X. Xu and Y. A. Abassi, *Anal Chem*, 2006, **78**, 35-43.
15. J. Meshki, S. D. Douglas, J. P. Lai, L. Schwartz, L. E. Kilpatrick and F. Tuluc, *J Biol Chem*, 2009, **284**, 9280-9289.
16. S. Seto, A. Tanioka, M. Ikeda and S. Izawa, *Bioorg Med Chem Lett*, 2005, **15**, 1479-1484.
17. M. F. Peters and C. W. Scott, *J Biomol Screen*, 2009, **14**, 246-255.
18. P. Scandroglio, R. Brusa, G. Lozza, I. Mancini, R. Petro, A. Reggiani and M. Beltramo, *J Biomol Screen*, 2010, **15**, 1238-1247.
19. A. O. Watts, D. J. Scholten, L. H. Heitman, H. F. Vischer and R. Leurs, *Biochem Biophys Res Commun*, 2012, **419**, 412-418.
20. V. Perez, T. Bouschet, C. Fernandez, J. Bockaert and L. Journot, *Eur J Neurosci*, 2005, **21**, 26-32.
21. K. Solly, X. B. Wang, X. Xu, B. Strulovici and W. Zheng, *Assay Drug Dev Techn*, 2004, **2**, 363-372.
22. E. Thedinga, A. Kob, H. Holst, A. Keuer, S. Drechsler, R. Niendorf, W. Baumann, I. Freund, M. Lehmann and R. Ehret, *Toxicol Appl Pharm*, 2007, **220**, 33-44.
23. US-WO2005077104 A3 Pat., WO2005077104 A3, 2008.
24. J. A. Allen and B. L. Roth, *Ann Rev Pharmacol Toxicol*, 2011, **51**, 117-144.
25. M.-H. Wu, S.-B. Huang and G.-B. Lee, *Lab Chip*, 2010, **10**, 939-956.
26. S.-L. Tsai, Y. Chiang, M.-H. Wang, M.-K. Chen and L.-S. Jang, *Electrophoresis* 2014, Advanced Online (DOI: 10.1002/elps.201300591).
27. Y. M. Mishina, C. J. Wilson, L. Bruett, J. J. Smith, C. Stoop-Myer, S. Jong, L. P. Amaral, R. Pedersen, S. K. Lyman, V. E. Myer, B. L. Kreider and C. M. Thompson, *J Biomol Screen*, 2004, **9**, 196-207.
28. M. Roelse, N. C. A. de Ruijter, E. X. Vrouwe and M. A. Jongsma, *Biosens Bioelectron*, 2013, **47**, 436-444.
29. G. E. Slaughter, E. Bieberich, G. E. Wnek, K. J. Wynne and A. Guiseppi-Elie, *Langmuir*, 2004, **20**, 7189-7200.
30. F. Zhang, K. Sautter, A. M. Larsen, D. A. Findley, R. C. Davis, H. Samha and M. R. Linford, *Langmuir*, 2010, **26**, 14648-14654.
31. S. Meyburg, R. Stockmann, J. Moers, A. Offenhäusser and S. Ingebrandt, *Sensors and Actuators B: Chemical*, 2007, **128**, 208-217.
32. S. C. Shih, I. Barbulovic-Nad, X. Yang, R. Fobel and A. R. Wheeler, *Biosens Bioelectron*, 2013, **42**, 314-320.
33. J. Wegener, C. R. Keese and I. Giaever, *Exp Cell Res*, 2000, **259**, 158-166.
34. S. Cho, *BioChip J*, 2011, **5**, 327-332.
35. K. Hatanaka, A. A. Lanahan, M. Murakami and M. Simons, *PloS One*, 2012, **7**, e37600.
36. J. Wang, C. Wu, N. Hu, J. Zhou, L. Du and P. Wang, *Biosensors*, 2012, **2**, 127-170.
37. Y. Fang, *Int J Electrochem*, 2011, **2011**, 16.
38. M. Rocheville and J. C. Jerman, *Curr Opin Pharmacol*, 2009, **9**, 643-649.
39. R. McGuinness, *Curr Opin Pharmacol*, 2007, **7**, 535-540.
40. US-WO2007030686 A2 Pat., 2007.
41. M. Chachisvilis, Y. L. Zhang and J. A. Frangos, *Proc Natl Acad Sci*, 2006, **103**, 15463-15468.
42. T. Voets and B. Nilius, *EMBO J*, 2009, **28**, 4-5.
43. S. M. Radke and E. C. Alocilja, *Sensors J IEEE*, 2004, **4**, 434-440.
44. Y. A. Abassi, B. Xi, W. Zhang, P. Ye, S. L. Kirstein, M. R. Gaylord, S. C. Feinstein, X. Wang and X. Xu, *Chem Biol*, 2009, **16**, 712-723.
45. J. Vazquez-Prado, H. Miyazaki, M. D. Castellone, H. Teramoto and J. S. Gutkind, *J Biol Chem*, 2004, **279**, 54283-54290.
46. P. Seriburi, S. McGuire, A. Shastry, K.F. Bohringer and D.R. Meldrum, *Anal. Chem*, 2008, **80**, 3677-3683.

47. M. Kammermann, A. Denelavas, A. Imbach, U. Grether, H. Dehmlow, C.M. Apfel and C. Hertel, *Biochem. Biophys. Res. Commun*, 2011, **412**, 419-424.